Modeling Uncertainty for a Vision System Applied to Vibration Measurements

Alberto Lavatelli[1], *Member, IEEE*, and Emanuele Zappa[2], *Member, IEEE*

[1]*Department of Mechanical Engineering, Politecnico di Milano, Milan 20133, Italy (e-mail: alberto.lavatelli@polimi.it).*
[2] *Department of Mechanical Engineering, Politecnico di Milano, Milan 20133, Italy (e-mail: emanuele.zappa@polimi.it)*

ABSTRACT In this paper, a new analytical model is proposed to describe the behavior of uncertainty for a generic vision-based measurement system applied to mechanical vibration measure-ment. In particular, this paper proposes a novel way to evaluate the effects of motion blur. The theoretical framework presented here takes into account the camera acquisition parameters, the dynamics of the measurand (in terms of instantaneous speed), and the image scaling factor to develop a physical model of uncertainty when measuring a mainly monomodal vibration. Uncertainty is evaluated starting from the normalized discrep-ancy between a measured position and the actual one. The analytical model proposed here has been validated extensively with the help of a test stand that can generate biaxial monomodal vibrations. The motion of a target mounted on the test stand has been simultaneously monitored by a stereo vision rig and a set of triangulation lasers. Model validation has been carried out using two measurement techniques: stereo vision blob analysis and digital image correlation. The experimental results show that the proposed model is able to represent the behavior of uncertainty for both the techniques. After the model has been validated, it is shown how it is possible to exploit it to estimate the uncertainty of a vision rig starting from the nominal characteristics of both the vision system and the target. This can be a tool to facilitate the design of vision-based measurement systems.

Index Terms— Dynamic measurements, experimental valida-tion, theoretical model, uncertainty, vibrations, vision systems.

I. Introduction

VISION-BASED measurements represent a wide variety of contactless techniques that are able to obtain data from an image-recorded scene with the help of digital cameras.
The goal of this paper is to provide a theoretical uncertainty model for a vision system applied in the context of vibration measurements. This model will take into account two main sources of uncertainty:

1) the spatial discretization introduced by digital imaging sensors and the characteristic size of the target;
2) the effect of the relative motion between the measurand and the camera, also known as *motion blur*.

As for issues related to spatial discretization, this research relies on scientific literature. Conversely, for the effects of motion blur, a novel model is proposed to evaluate the accuracy of a measurement system from the physical description of the measurement procedure. Therefore, this paper focuses on those sources of uncertainty that are common to all vision system applications, regardless of the specific measurement methodology.
In fact, although every measurement method interprets acquired images in its own particular way, the process of shooting a marker or a speckle applied to a moving target is the same. Thus, the most diffused vision systems share a common source of uncertainty and, although the final accuracy of a measurement system depends heavily on the particular mea-suring methodology, the phenomena are expected to behave similarly.

Manuscript received November 2, 2015;
revised December 28, 2015;
accepted February 24, 2016. Date of publication
March 29, 2016.

II. State of the Art

The application of vision systems has become a topic of broad interest throughout the scientific community. Furthermore, during the last decade the development of more performing devices at diminishing costs has expanded the field of application of vision systems, making them an attractive and valuable solution for both scientific research and industrial applications.

In particular, the possibility to provide contactless monitoring and the relatively easy setup (no need to access critical areas to fix transducers) push the diffusion of those systems. Furthermore, when using a camera for displacement measurements, every row or column in the pixel matrix can be considered a sensor on its own. For this reason, cam-eras are usually referred to as *dense* sensors. Unfortunately, cameras show several limitations that can be grouped as follows.

1) *Optical System Limitations [1]:* Since cameras are opti-cal devices affected by problems such as distortion and aberration.
2) *Bandwidth Limitations [2]:* Since it takes a finite time for an image to be generated and then transmitted to the computer.
3) *Image Processing Limitations [3]:* Since images carry, in general, a large amount of data that need a finite time to be processed.
4) *Lighting Limitations [4]:* Since for image-based mea-surements the information is carried by light, and hence, it may be difficult to use vision techniques in applica-tions where lighting is constrained.
5) *Resolution Limitations [5]:* Since the field of view is discretized with a finite number of pixels.

In order to overcome the aforementioned limitations, significant effort has been invested by the scientific community in researching and modeling the uncertainty over the years. In the early days, research work was focused on model-ing the contribution of the relative position and orientation of the vision rig to the development of uncertainty [6]. Then the attention of the machine vision community focused on the sources of uncertainty correlated with calibration [7]; in particular, the formulation of uncertainty for the fundamen-tal matrix of epipolar transformation was investigated [8], [9].

The efforts made in understanding uncertainty clearly showed the need for newer and more effective calibration procedures. Thus, during the late 1990s, several innovative calibration algorithms were proposed [10]–[12] to reduce uncertainty. The final outcome of that research period is the Zhang calibration algorithm [13], which, until now, was considered a benchmark in the generic calibration of vision systems. Starting from 2000, most investigations into uncertainty have been focused on the image segmentation problem. Conse-quently, innovative feature-matching algorithms [14], [15] capable of identifying homographies with less uncertainty [16] were defined.

While most of the engineering community had been busy with the enhancement of classic vision systems, other researchers started to look for different ways of measuring displacement using cameras. In this field, the contributions of Sutton, Luo, and Chao are remarkable since, during the early 1990s, they provided the scientific community with the digital image correlation (DIC) technique [17], [18]. The emer-gence of DIC meant the availability of full-field measurements rather than just a point measurement.

DIC is also affected by uncertainties. In general, the work done on the classic stereo vision for the uncertainties related to the position and orientation of the vision rig, optical phenomenon, and calibration applies in the same way to DIC [19]. However the study of uncertainty related to the DIC measuring algorithm needs a specific field of research. In fact the DIC methodology benefits from the use of dedicated shape functions to describe the transformation that occurs to a reference speckle subjected to deformation and displacement. These shape functions are able to represent only predefined kinematics and not all the possible transformations. This situation generates systematic uncertainties [20].

The displacement and strain fields returned by DIC are obtained after a procedure of error minimization that is affected by uncertainty. Hence, the scientific community devoted efforts to understanding the role played by noise in motion reconstruction [21], [22]. These studies have clearly demonstrated the relation between the shape of the speckle and the uncertainty connected with noise and pattern mismatch. More recently, a field of research has been dedicated to the optimal design of speckles [23]. Another important research field in the context of DIC is the preprocessing of acquired images in order to minimize uncertainty [24].

A. Focus on the Application to Vibration Measurements

The use of imaging devices as displacement transducers was first proposed in almost-static applications, where the effect of target motion during the exposure time can be neglected.

Thanks to advances in technology, the application of vision-based measurement to dynamic conditions has been increas-ing recently. The available image resolutions and the high grabbing frequencies make it possible to acquire high-speed moving objects and to perform dynamic analysis of vibrating objects [25].

The quantification of the measurement of uncertainty using imaging devices in dynamic conditions becomes more complex in the static case. The final uncertainty value is composed by the parameters listed before and the contribute due to the relative motion between camera and target (in terms of instantaneous velocity and acceleration) [26].

Good displacement estimation will indeed depend on the dynamic camera parameters, such as grabbing frequency, but, most of all, on the exposure time that must be set to an appropriate value in order to limit the phenomenon of motion blur.

For these reasons, many researchers have found a good solution by boosting the lighting and selecting very low exposure times to shoot the vibrating object in approximately static conditions [27]. Unfortunately, it is not possible to follow these conditions in all measurement tasks. For instance, in the relevant field of structure monitoring, the application of the vision measurement system often requires to work with natural light [28]. Therefore, the exposure time cannot be set arbitrarily; hence, it plays a relevant role, and the source of uncertainties peculiar to dynamic measurements starts to be relevant [29].

In conclusion, a history of a wide variety of applications clearly indicates that modeling of uncertainty in dynamic conditions implies the understanding of the role played by the interaction between the exposure time and the velocity of the vibrating object [30].

III. ANALYTICAL MODEL FOR UNCERTAINTY IN DYNAMIC CONDITIONS

In order to analytically model uncertainty when measuring the position of a vibrating item, it is necessary to formulate a simple scheme. In this case, let us consider the following:

1) a marker of characteristic dimension L_0, moving monodimensionally in the pixel space with law $x(t) = A_0 \cdot \sin(\omega t)$;
2) an image acquisition device that discretizes space with space resolution Δx;
3) an image acquisition device that acquires images with a finite exposure time t_{sh};
4) an image processing technique that measures motion as the center of gravity of the transverse luminance profile of the marker.

Given this setup, it is possible to show the following quantities.

1) The position of the marker barycenter at the start of the exposure $x_r(t_0)$, which represents the reference position.
2) The marker position as measured by means of image processing $x_{meas}(t_0)$. In this case, the exposure starts at t_0 and ends at $t = t_0 + t_{sh}$.

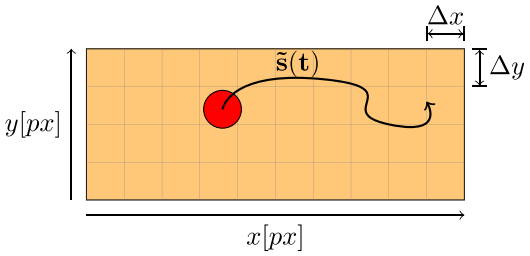

Fig. 1. Simple scheme of spatial discretization.

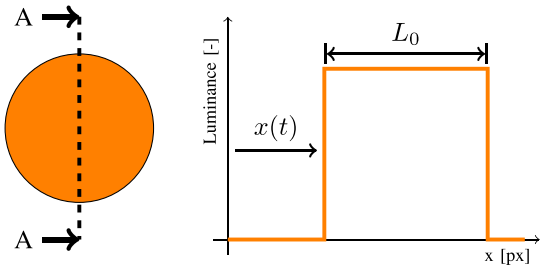

Fig. 2. Transverse luminance profile $M(x)$ of the marker.

3) The discrepancy between the reference position and the measured one is $\Delta A = x_{\text{meas}}(t) - x_r(t)$.
4) The normalized discrepancy is $\varepsilon = (\Delta A / x_r(t))$.

A. Sources of Uncertainty

It is known that in the application of imaging techniques to moving targets, two sources of uncertainty are relevant.

1) A static component [31] due to spatial discretization.
2) A dynamic component [32] generated by the interaction of the marker motion with the acquisition time that is, by definition, finite. This component is known as *motion blur*.

Other contributions to uncertainty (extrinsic parameters of a stereoscopic system, optical aberration, noise, etc.) are not modeled by the theoretical construction presented here. However, these sources of uncertainty may be further included in the static component since, in general, they do not depend on the motion of the measurand.

B. Static Component: Space Discretization

As regards uncertainty due to spatial discretization, the process is modeled as a linear discretization of actual motion metrics into pixels, as shown in Fig. 1.

In particular, let us consider a marker lying steady in a generic position on the x-axis. In this case, the real position of the center of gravity $x_r(t)$ is constant and identically equal to x_0.

Given the steady state of the marker, the exposure time does not play any role in this situation. Hence, it is possible to express the measured position of the marker as

$$x_{\text{meas}} = x_0 \pm \frac{\Delta x}{2}. \tag{1}$$

Furthermore, it is possible to calculate the discrepancy between the measured position and the actual one as

$$\Delta A = x_{\text{meas}}(t) - x_r(t) = \pm \frac{\Delta x}{2}. \tag{2}$$

Given the result of (2), it is possible to consider a situation where the images of the measurand moving with law $x(t) = A_0 \cdot \sin(\omega t)$ are acquired with infinitesimal shutter times. In this case, motion blur does not appear; hence, it is possible to calculate the static component of normalized discrepancy as a function of motion amplitude

$$\varepsilon_S(A_0) = \frac{\Delta A}{A_0} = \frac{\Delta x}{2 \cdot A_0}. \tag{3}$$

This result is proposed as a theoretical construction based on the linear signal sampling theory and without loss of generality. In fact, for any kind of vision measurement methodology (even subpixel methods), it is possible to identify a certain limit of resolution that the proposed model resembles.

C. Dynamic Component: Motion Blur

When the images of a moving marker are acquired, motion blur is generated. The effect of the blur can be either significant or negligible, and in any case, the phenomenon can be modeled using the signal convolution theory, as shown in [32] and [33].

As we are considering a monodimensional motion, it is possible to evaluate the marker shape deformation by considering its longitudinal cross section $M(x)$ as shown in Fig. 2. Thus, the 2-D signal acquisition can be treated as a monodimensional problem, using 1-D convolution signal processing application [34].

Hence, it is possible to model the deformation of signal $M(x)$ in dynamic conditions as a result of the convolution between the motion $x(t)$ with the acquisition window $w(t)$, so that the deformed profile $M'(x)$ is generated by

$$M'(x) = (M * w)(x) = \int_0^x M(X) \cdot w(X - x) dX. \tag{4}$$

The acquisition window $w(x)$ should be calculated after the marker motion $x(t)$ and its first derivative with respect to the time $\dot{x}(t)$. A general solution is not retrievable; however, it is possible to circumvent the problem with the help of the following statements.

1) Vibrational motion is considered in the form of $x(t) = A_0 \cdot \sin(\omega t)$.
2) The exposure begins at the generic time $t = t_0$, which leads to the initial position $x_0 = A_0 \cdot \sin(\omega t_0)$.
3) Let us consider exposure time $t_{\text{sh}} \ll (2\pi/\omega)$.
4) As a result of points 2 and 3, it is possible to linearize the motion during shutter with the following, where V_0 represents the modulus of velocity at the beginning of shutter:

$$\begin{cases} x(t - t_0) \approx x_0 + \text{sgn}(\dot{x}) \cdot V_0 \cdot (t - t_0) \\ V_0 = |\dot{x}(t_0)| = |A_0 \omega \cdot \cos(\omega t_0)|. \end{cases} \tag{5}$$

Now it is possible to describe the acquisition window as a rectangular pulse of length q_0. The window length is then estimated by

$$q_0 = V_0 \cdot t_{\text{sh}} = |A_0 \omega \cdot \cos(\omega t_0)| \cdot t_{\text{sh}}. \tag{6}$$

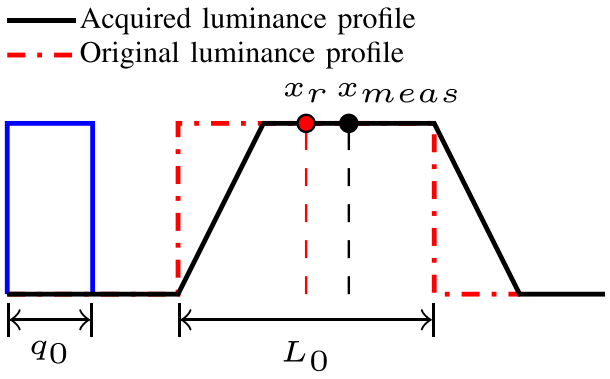

Fig. 3. Effect of convolution phenomenon on marker luminance profile.

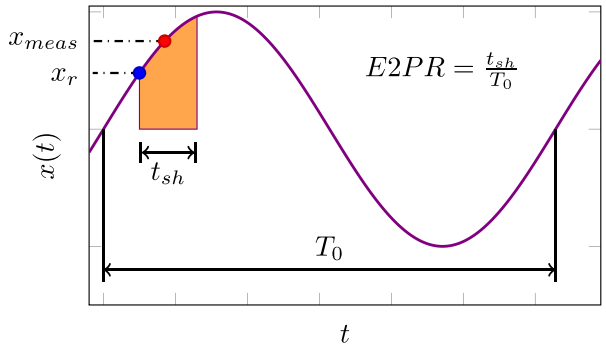

Fig. 4. Effect of measurand motion during exposure on the calculation of marker position.

Therefore, it is possible to calculate exactly the output of the convolution process $M'(x)$, since it is the mobile average processing of the marker profile $M(x)$, as shown in Fig. 3. Furthermore, both the original and the deformed profiles are geometrical shapes, respectively, a rectangle and a trapezoid.

The consequence of the convolution process is that the initial rectangular signal is deformed into a trapezoid. It is possible now to calculate the center of gravity of each signal, which represents the actual measurement as stated before. With reference to Fig. 3, the quantities x_r and x_{meas} are calculated as follows:

$$\begin{aligned} x_r &= x_0 + \frac{L_0}{2} \\ x_{\text{meas}} &= x_0 + \frac{L_0}{2} + \frac{q_0}{2} \cdot \text{sgn}(\dot{x}). \end{aligned} \tag{7}$$

From a graphical point of view, as shown in Fig. 4, the convolution process leads to an overestimation (or underestimation if $\dot{x} < 0$) of the marker motion.

Given the values retrieved in (7), it is possible to calculate the following quantities:

1) discrepancy $\Delta A = x_{\text{meas}} - x_r = (q_0/2) \cdot \text{sgn}(\dot{x})$;
2) normalized discrepancy $\varepsilon = (\Delta x / x_r)$.

Now it is necessary to substitute into the formula of ε the values retrieved in (7)

$$\varepsilon = \frac{\Delta A}{x_r} = \frac{q_0}{2x_0 + L_0} = \frac{V_0 \cdot t_{\text{sh}} \cdot \text{sgn}(\dot{x})}{2x_0 + L_0}. \tag{8}$$

Then given $\phi_0 = \omega_0 \cdot t_0$, by recalling expression (6), it is possible to write

$$\varepsilon = \frac{V_0 \cdot t_{\text{sh}}}{2x_0 + L_0} = \frac{A_0 \omega_0 \cdot \cos(\phi_0) \cdot t_{\text{sh}}}{2A_0 \cdot \sin(\phi_0) + L_0}. \tag{9}$$

It is interesting to analyze in detail the numerator of (9). In fact it is possible to write $\omega_0 = (2 * \pi / T_0)$, where T_0 is the period of $x(t)$. Therefore, the product $\omega_0 \cdot t_{\text{sh}}$ is proportional to the ratio between the shutter time and the period of motion. The value of the aforementioned ratio is identified as a distinctive parameter of every vision technique applied to dynamic measurements. Thus, the parameter E2PR [26] is now introduced as

$$\text{E2PR} = \frac{t_{\text{sh}}}{T_0} = t_{\text{sh}} \cdot f_0. \tag{10}$$

Now it is possible to write the final expression of normalized discrepancy due to the dynamic factors ε_D, by substituting (10) into (9)

$$\varepsilon_D = \frac{A_0 \cdot \cos(\phi_0) \cdot 2\pi \cdot \text{E2PR}}{2A_0 \cdot \sin(\phi_0) + L_0}. \tag{11}$$

D. General Uncertainty Model

From the foregoing discussion, it is possible to provide a formulation for discrepancy dynamics for the general vision system applied to monodimensional motion.

As stated before, two phenomena contribute to the development of discrepancies between the actual motion and the measured one: a static uncertainty due to spatial discretization and a dynamic discrepancy due to the sampling window necessary to achieve time discretization.

The static contribution $\varepsilon_S(A_0)$ is modeled by (3), while the dynamic contribution $\varepsilon_D(A_0)$ is modeled by (9). In (9), the amplitude A_0 is expressed in pixels, while in (3), it is measured in millimeters. In order to match the two equations mentioned here, the mm/pixel conversion factor Δx is used to retrieve the amplitude in pixels, without loss of generality. The two contributions can be combined linearly to generate the function $\varepsilon_T = \varepsilon_S(A_0) + \varepsilon_D(A_0)$ shown in

$$\begin{aligned} \varepsilon_T(A_0) &= \frac{\Delta x}{2 \cdot A_0} + \frac{A_0 \cdot \frac{1}{\Delta x} \cdot \cos(\phi_0) \cdot 2\pi \cdot \text{E2PR}}{2A_0 \cdot \frac{1}{\Delta x} \cdot \sin(\phi_0) + L_0} \\ &= \frac{k_0}{A_0} + k_1 \cdot \frac{A_0}{k_2 \cdot A_0 + k_3}. \end{aligned} \tag{12}$$

Expression (12) needs to be properly analyzed. In fact ε_S and ε_D show different trends when the motion amplitude A_0 increases; consequently, the behavior of the total amount of uncertainty ε_D needs to be investigated.

Having fixed all the factors k_i, in Fig. 5 the curve of $\varepsilon_D(A_0)$ is plotted together with its static and dynamic components. When the motion amplitude increases, the dynamic component of uncertainty is increased, while the static branch travels asymptotically to zero. From a physical point of view, the role of image resolution in motion reconstruction is less relevant when the amplitude of motion is far from the spatial discretization step. However, considering iso-frequent vibrations,

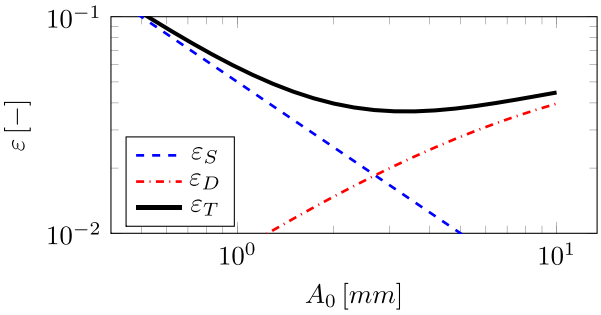

Fig. 5. Error behavior as a contribution of static and dynamic factors.

the bigger the amplitude, the bigger the instantaneous speed of the measurand during exposure time. Hence, the motion blur contributes significantly to the total amount of uncertainty when the vibration amplitude is increased.

Having the static branch decreasing with amplitude increasing and, conversely, the dynamic branch increasing, the total amount of uncertainty ε_D describes a bowel curve, with a minimum point where the two components intersect.

In conclusion, although the model presented here has been developed on a monodimensional basis, its validity extends to a generic n-dimensional motion measured by the orthogonal axis. In this case each axis is linearly independent; hence, it can be treated as a set of independent uncertainty parameters.

E. Model Applicability

Given the results highlighted above, it is necessary to clarify what the limits of applicability of the proposed model are in the description of an actual measurement system. In fact, vibrations are stochastic phenomena in the domains of time and frequency; nonetheless, the generic vibration phenomenon can be characterized by a combination of several harmonics and process noise. Vision systems are optoelectric systems affected by all the peculiar sources of uncertainty described in Section II.

The model presented in this paper can be used to analyze the behavior of vision-based measurement systems in the context of the following.

1) Mainly monomodal vibrations (both in 2-D and 3-D space for multiaxial monitoring).
2) Properly focused systems, because optical blurring (due to defocusing) should be negligible in comparison with motion blur. Otherwise, the amount of uncertainty due to defocusing overcomes the effects of motion blur.
3) Luminosity of the scene high enough to provide feature detection without image saturation.

The proposed model describes how the motion blur phenomenon interferes with the correct estimation of the geometrical features nested in the acquired images; hence, it applies to both 2-D and 3-D systems. Nowadays, vision measurement tasks are often carried out by means of 3-D imaging techniques; therefore, the authors focused their attention and validated the model in the 3-D case.

IV. Model Validation

In order to validate the model, a dedicated vibratory test stand has been designed. Vibrations have been provided by a cantilever beam having a rectangular section. In order to provide complex motion, beam flanks have been Computer Numerical Control (CNC) milled to obtain two different moments of inertia of the beam sections along the two transverse axes. The amount of milling had been selected with the help of a FEM simulation in order to provide two different values of natural frequencies f_y and f_x: 21.6 and 22.9 Hz, respectively, for the y- and x-axes. The FEM predictions have then been experimentally verified with accelerometers during the test-stand installation.

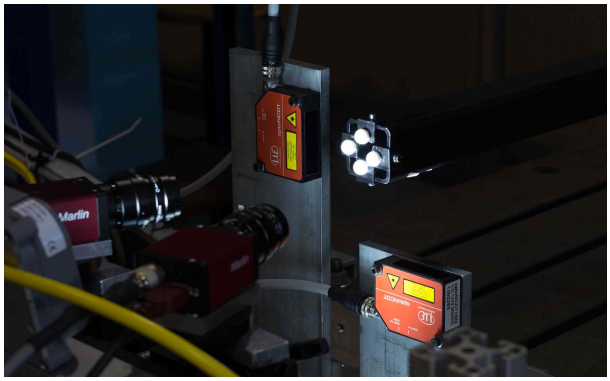

Fig. 6. Test stand used for model validation. The beam tip is equipped with SVBA markers, triangulation lasers, and cameras.

The free end of the vibrating beam has been equipped with a system capable of carrying both a DIC speckle and a set of 4 spherical markers for stereo vision blob analysis (SVBA). In fact, given the generic formulation of the model of (12), the theoretical frame proposed here is capable of handling both the techniques.

The motion of the beam tip is measured by a stereo vision rig consisting of two AVT Marlin F131B cameras (focal length of 8 mm according to ISO 517) mounted on a stiff aluminum frame together with dimmerable LED lighting (Smart Vision Lights ODS75) and two triangulation lasers ($\mu\varepsilon$ OptoNCDT 1302-50) aligned with the cantilever beam, as shown in Fig. 6. The performances of the electro-optical setup have been evaluated from the 0, 10SFR response level according to the ISO 12233 standard [35], showing a sampling efficiency rating of $E_s = 91\%$. Images have been transferred to the PC using the IEEE 1394 bus and stored in IEEE 12234-compliant TIFF files.

In this way the beam tip displacement is monitored by two measurement systems. In particular, the uncertainty of the vision system is judged over the reference measurement offered by triangulation lasers, which are affected by negligible uncertainty with respect to the stereo vision rig used [36].

The experimental validation had been carried out by means of decay tests, where the beam tip had been first excited, and then slowed down by natural damping. In this situation, motion amplitudes and the discrepancy between the lasers and the vision systems have been calculated from raw signals with the help of rms windowing (length 1100 ms in order to accommodate about 25 periods, 500 ms overlap). Consequently, the ratio between the discrepancy and the laser amplitude returns several data points of the normalized discrepancy ε as

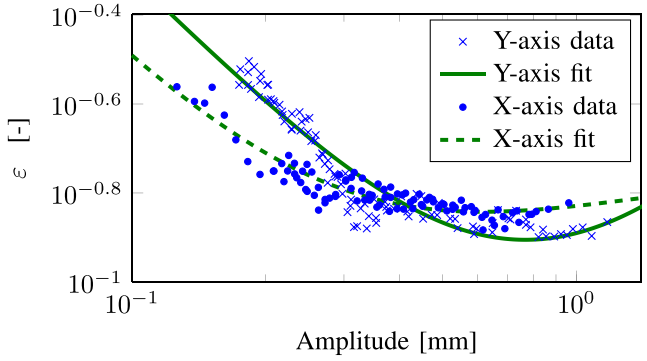

Fig. 7. Fitting experimental data with physical model. Test at E2PR ≈ 0.092 with SVBA.

TABLE I

TESTING PATH INVESTIGATED DURING VARIABLE SHUTTER EXPERIMENTS

Test id	Shutter value [-]	Exposure time $[ms]$	E2PR [-]
#1	20	0.4	0.008
#2	40	0.8	0.017
#3	220	4.4	0.092
#4	320	6.4	0.134
#5	420	8.4	0.176
#6	620	12.4	0.260
#7	750	15	0.315
#8	850	17	0.357
#9	1000	20	0.420

a function of the displacement amplitude for a single testing condition.

The acquired data points $\varepsilon_i(A_i)$ are then fitted with the model of (12) in order to validate the physical nature of the theory proposed here.

As can be seen in Fig. 7, the theoretical model represents the physical reality. As expected, the curve of the normalized discrepancy draws a minimum point at a given value of amplitude. During the tests, the natural frequency of motion and the range of motion amplitudes under investigation had been kept constant. Conversely, all the acquisition parameters (shutter, lighting, and frame rate) and the shape of markers/speckles have been changed throughout the testing activity. Hence, model validation has been pursued by monitoring the reaction of the model to changes in E2PR and the marker characteristic dimension L_0.

A. Tests at Variable Shutter With SVBA

In this section, the effect of changes in the exposure time is investigated. The model of uncertainty formulated in (11) predicts an increasing trend for the uncertainty as the E2PR parameter increases. Consequently, the experiment presented here had been designed to evaluate the truthfulness of the previous assumption. The experimental conditions are shown in Table I. The experiments had been conducted by regulating the level of lighting together with the shutter in order to keep the level of luminance of the acquired images constant (the higher the exposure, the lower the lighting). In this way, the effectiveness of the segmentation/correlation algorithms is not influenced by changes in the exposure time. The maximum

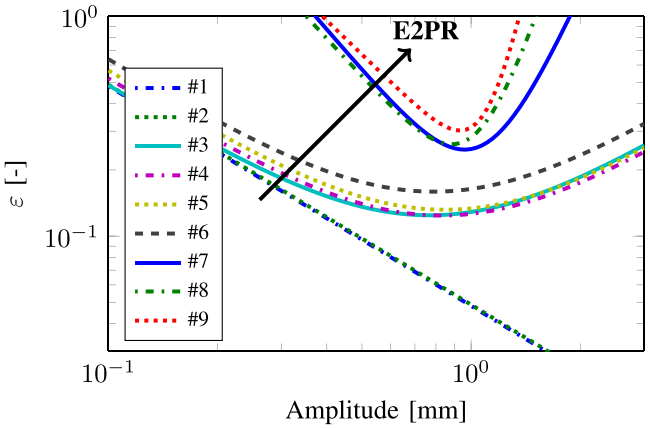

Fig. 8. Aggregate results of variable shutter test on SVBA for the y-axis. Data of each test have been fitted with the model of (12).

amount of motion blur (in terms of convolution window width) tested during the experimental path is about 11 px.

For each shutter level, four acquisitions of 20.4 s have been considered for fitting purposes, in order to accommodate more than 400 periods for each acquisition. Each data set had to be fitted by the model of (12) and the fit was accepted only if the R^2 parameter was higher than 0.92 and only if the residuals fulfilled the Anderson–Darling normality test [37]. Otherwise, the fit was rejected and the run had to be repeated. During the tests, 5 runs out of 41 were discarded due to electromagnetic noise affecting the lasers' signal. Consequently, each shutter setup has been investigated with a total amount of 81.6 s of acquisition, which means more than 1600 periods monitored for each shutter value. The whole variable shutter experiment included the acquisition of 36 runs, 734 s of acquisition, and more than 14 400 periods overall.

As can be seen in Fig. 8, at low E2PR there is no evidence of uncertainty growing with the vibration amplitude; hence, a quasi-static mode is identified. Then, as the shutter increases, the uncertainty displays a dynamic behavior and discrepancies become more relevant. At even higher values of E2PR, the system behaves with a really high uncertainty due to the complete corruption of images caused by motion blur.

Eventually, the results displayed here confirm the sensitivity of vision systems to E2PR and, at the same time, they validate the assumption that uncertainty grows together with E2PR.

B. Tests at Fixed Lighting Conditions With SVBA

A second model validation has been carried out by simulating a typical situation of outdoor measurements, where the lighting is fixed and set with natural light. In fact, in this test the lighting has been fixed, while the effect of the shutter on the accuracy has been investigated by monitoring the average value of the normalized discrepancy (indicated with the symbol ε_{av}) throughout each test.

As can be seen in Fig. 9, the average value of discrepancy diminishes when E2PR is lowered. However, for very low E2PR values, uncertainty rises again, since the images become too dark for accurate processing. Eventually, when operating in fixed light conditions, it is possible to find an optimal value of E2PR.

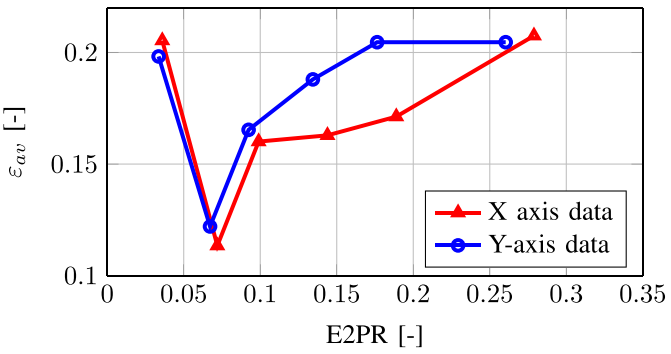

Fig. 9. Behavior of uncertainty at fixed lighting conditions as E2PR changes.

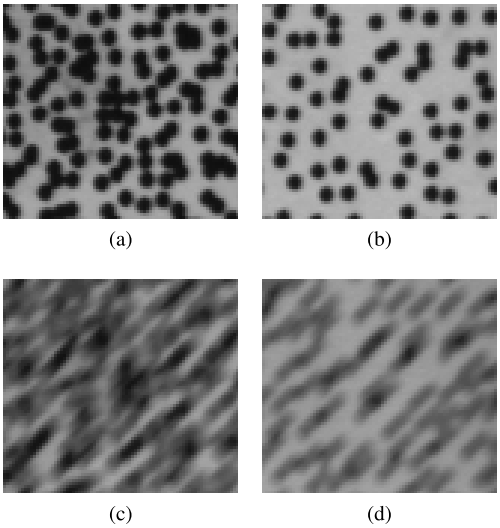

Fig. 10. Two speckles used for experiments at variable characteristic dimensions. Pattern D6 in steady conditions (a) and in motion blurred conditions (c). Pattern D9 in steady conditions (b) and in motion blurred conditions (d).

C. Tests at Variable Characteristic Dimension With DIC

The last model validation section investigates the role played by the marker characteristic dimension L_0 in generating uncertainty in dynamic conditions. In this case, the beam tip had been equipped with a DIC speckle to monitor vibrations.

As shown in Fig. 10, two different dotted patterns have been tested. The first pattern (identified as the D6 pattern; an average in-center spacing of 6 px and a dot size of 4.5 px) was a speckle optimized for static dense measurements [24], [38], [39]; hence, it was filled with a fine mesh grid of black points on a white background. The second pattern (identified as the D9 pattern; an average in-center spacing of 9 px and a dot size of 4.5 px) had a wider in-center spacing in order to reduce the overlap of the motion blur stripes for each speckle (as shown in Fig. 10). In particular, it is necessary to highlight the difference between the two values of fill coefficient (identified by the ratio between the area covered by dots and the background): 0.49 for D6 and 0.21 for D9.

In Fig. 11, a comparison between the performances of the two speckles is shown with both experimental data and the fitting with the proposed model. It can be seen that the

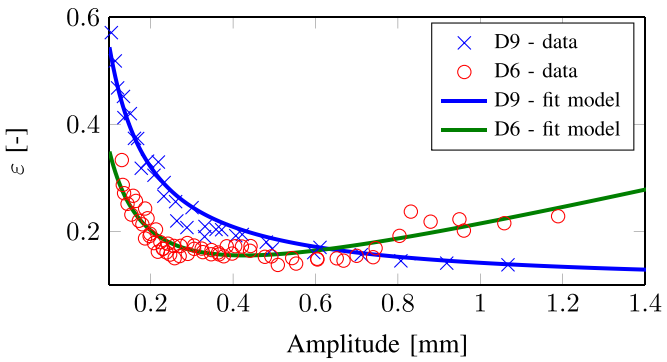

Fig. 11. Comparison between the performances of an optimized DIC pattern (D6) and a coarser one (D9).

D6 speckle behaves with low uncertainty in static conditions since it has been designed on purpose. At the same time, the D6 pattern appears to be really sensitive to the effects of motion blur with discrepancy developing fast with the instantaneous speed of the measurand increasing. In fact, due to the small in-center spacing, even a small amount of motion blur can corrupt images due to overlapping of the speckle's stripes.

Conversely, the D9 pattern, as predicted by the model, is less sensitive to the effects of motion blur and still displays a quasi-static behavior. Nevertheless, given the lower density of speckles, the static performances worsen in comparison with the D6 pattern.

In conclusion, the last experiment validates the predictions offered by the model proposed earlier. In particular, it has been demonstrated that increasing the marker characteristic dimension (i.e., the average in-center spacing of the features) reduces the sensitivity to uncertainties generated by motion blur.

V. Model-Based Vision Rig Design

Once the model has been extensively validated, it can be used to characterize a vision rig dedicated to dynamic displacement measurement such as vibration measurement or tracking of moving objects.

First, it is possible to approximate the parameters used in (12) from the nominal characteristic of a vision rig. In fact, both the pixel/mm conversion and the characteristic dimension of marker can be estimated using the pin-hole camera model [40]. At the same time, E2PR can be calculated once the exposure time t_{sh} and the frequency of vibration are known.

The phase of motion ϕ_0, instead, is to be determined. Let us consider an rms window that contains $N \gg 1$ cycles. Given that the motion blur depends on the modulus of velocity V_0, it is necessary to calculate the average value of V_0 inside the rms window.

Considering a situation where the target is monitored with a sample rate that is not an integer multiple of motion frequency, the instants of sampling are randomly uniformly distributed within the period of motion. In this case, it can be demonstrated that the average value of the modulus of

TABLE II

NOMINAL DATA WITH THEIR RELATIVE UNCERTAINTY USED TO ESTIMATE THE PERFORMANCE OF THE SYSTEM

Quantity	Δx	t_{sh}	f_y	L_0
Unit	$\left[\frac{mm}{px}\right]$	$[ms]$	$[Hz]$	$[px]$
Value	$0.1 \pm 2\%$	$8.4 \pm 10\ \mu s$	$21.6 \pm 2\%$	$83 \pm 1.5\%$
PDF	Normal	Uniform	Normal	Uniform

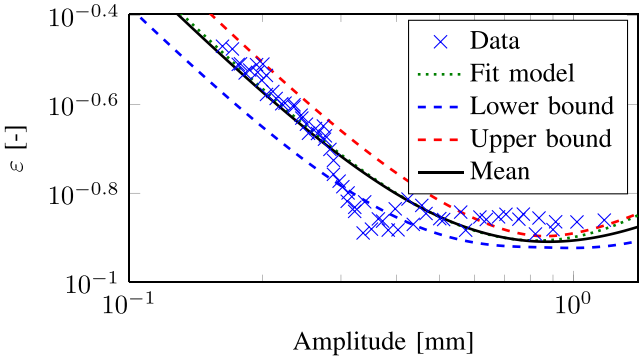

Fig. 12. Comparison between the fitted model and the approximated one for a test with SVBA, y-axis, E2PR = 0.18. Approximated model is displayed together with 95% confidence bounds.

velocity V_0 corresponds to the instantaneous velocity at the phase $\phi = \cos^{-1}(2/\pi) = 50.45°$. Hence, for the purposes of this discussion, the phase ϕ_0 is identically equal to 50.45°.

In the case of the SVBA setup used within this research work, the uncertainty parameters k_i are estimated from the nominal data displayed in Table II. Values, uncertainties, and probability density functions (PDFs) are retrieved from different sources: Δx and L_0 from camera calibration, t_{sh} from camera datasheet, and f_y from modal analysis.

With the help of the Monte Carlo framework, it is possible to sample nominal values from their PDFs. Consequently, it is possible to estimate for each value of vibration amplitude a PDF for the value of the normalized discrepancy ε. Then, the PDF is used to calculate the expected value of ε and its relative lower and upper confidence bounds. As can be seen in Fig. 12, this process leads to a fairly good prediction of the behavior of uncertainty. In fact, the approximated model lies close to the data and to the fitted curve as well.

As a consequence, it is possible to exploit the procedure proposed here to critically select the hardware of a vision system starting from the datasheet of its components. Another possibility is to optimize the acquisition parameters under a certain constraint (i.e., choosing an E2PR acceptability range in order to grant a desired level of accuracy).

VI. CONCLUSION

After a wide bibliographic research, this paper proposes a new physical model that describes the effect of motion blur on the behavior of uncertainty when applying a generic vision-based measurement system to vibration measurements.

The model presented here exploits the mathematical tool of convolution product to formulate a theory that describes the generation of discrepancies between a real motion and that acquired by a generic vision system. In particular, it is described how the exposure time and the relative motion between camera and target affect the shape of the features.

The theory proposed here has been submitted for experimental validation with two different stereovision measurement techniques: SVBA and DIC. The experimental results showed the validity of the proposed model for both the techniques.

In the end, it has been possible to propose a model-based design of vision rigs, where the theoretical model presented here can be used to select the optimal components and parameters for a vision system.

REFERENCES

[1] R. Sirohi, *Optical Methods of Measurement: Wholefield Techniques*, 2nd ed. Boca Raton, FL, USA: CRC Press, 2009.

[2] M. Huang, O. Serres, S. Lopez-Buedo, T. El-Ghazawi, and G. Newby, "An image processing architecture to exploit I/O bandwidth on reconfigurable computers," in *Proc. 4th Southern Conf. Program. Logic*, Mar. 2008, pp. 257–260.

[3] P. Zhang, J. Zhang, H. Deng, and L. Yu, "3D reconstruction for sinusoidal motion based on different feature detection algorithms," *Proc. SPIE*, vol. 9446, pp. 94463L-1–94463L-8, Mar. 2015.

[4] R. Gallen, A. Cord, N. Hautière, É. Dumont, and D. Aubert, "Nighttime visibility analysis and estimation method in the presence of dense fog," *IEEE Trans. Intell. Transp. Syst.*, vol. 16, no. 1, pp. 310–320, Feb. 2015.

[5] G. Busca, A. Cigada, A. Manenti, and E. Zappa, "Vision-based measurements for slender structures vibration monitoring," in *Proc. IEEE Workshop Environ., Energy, Struct. Monitor. Syst. (EESMS)*, Sep. 2009, pp. 98–102.

[6] E. Grosso, G. Sandini, and M. Tistarelli, "3D object reconstruction using stereo and motion," *IEEE Trans. Syst., Man, Cybern.*, vol. 19, no. 6, pp. 1465–1476, Nov./Dec. 1989.

[7] S. Das and N. Ahuja, "Performance analysis of stereo, vergence, and focus as depth cues for active vision," *IEEE Trans. Pattern Anal. Mach. Intell.*, vol. 17, no. 12, pp. 1213–1219, Dec. 1995.

[8] G. Di Leo, C. Liguori, and A. Paolillo, "Covariance propagation for the uncertainty estimation in stereo vision," *IEEE Trans. Instrum. Meas.*, vol. 60, no. 5, pp. 1664–1673, May 2011.

[9] G. Csurka, C. Zeller, Z. Zhang, and O. D. Faugeras, "Characterizing the uncertainty of the fundamental matrix," *Comput. Vis. Image Understand.*, vol. 68, no. 1, pp. 18–36, Oct. 1997.

[10] M. A. Sid-Ahmed and M. T. Boraie, "Dual camera calibration for 3-D machine vision metrology," *IEEE Trans. Instrum. Meas.*, vol. 39, no. 3, pp. 512–516, Jun. 1990.

[11] S. Lee and S. Ro, "A self-calibration model for hand-eye systems with motion estimation," *Math. Comput. Model.*, vol. 24, nos. 5–6, pp. 49–77, Sep. 1996.

[12] R. Benosman, T. Manière, and J. Devars, "Panoramic sensor calibration," *Pattern Recognit. Lett.*, vol. 19, nos. 5–6, pp. 483–490, Apr. 1998.

[13] Z. Zhang, "A flexible new technique for camera calibration," *IEEE Trans. Pattern Anal. Mach. Intell.*, vol. 22, no. 11, pp. 1330–1334, Nov. 2000.

[14] C. F. Olson, "Maximum-likelihood image matching," *IEEE Trans. Pattern Anal. Mach. Intell.*, vol. 24, no. 6, pp. 853–857, Jun. 2002.

[15] C. Doignon, D. Knittel, and X. Maurice, "A vision-based technique for edge displacement and vibration estimations of a moving flexible Web," *IEEE Trans. Instrum. Meas.*, vol. 57, no. 8, pp. 1605–1613, Aug. 2008.

[16] S. Se, D. Lowe, and J. Little, "Mobile robot localization and mapping with uncertainty using scale-invariant visual landmarks," *Int. J. Robot. Res.*, vol. 21, no. 8, pp. 735–758, 2002.

[17] M. A. Sutton, T. L. Chae, J. L. Turner, and H. A. Bruck, "Development of a computer vision methodology for the analysis of surface deformations in magnified images," in *Proc. ASTM Int. Adv. Video Technol. Microstruct. Control*, vol. 1094. 1991, pp. 109–132.

[18] P. F. Luo, Y. J. Chao, M. A. Sutton, and W. H. Peters, III, "Accurate measurement of three-dimensional deformations in deformable and rigid bodies using computer vision," *Experim. Mech.*, vol. 33, no. 2, pp. 123–132, 1993.

[19] P. Lava, W. Van Paepegem, S. Coppieters, I. De Baere, Y. Wang, and D. Debruyne, "Impact of lens distortions on strain measurements obtained with 2D digital image correlation," *Opt. Lasers Eng.*, vol. 51, no. 5, pp. 576–584, 2013.

[20] H. W. Schreier and M. A. Sutton, "Systematic errors in digital image correlation due to undermatched subset shape functions," *Experim. Mech.*, vol. 42, no. 3, pp. 303–310, 2002.
[21] Z. Y. Wang, H. Q. Li, J. W. Tong, and J. T. Ruan, "Statistical analysis of the effect of intensity pattern noise on the displacement measurement precision of digital image correlation using self-correlated images," *Experim. Mech.*, vol. 47, no. 5, pp. 701–707, 2007.
[22] Y. Q. Wang, M. A. Sutton, H. A. Bruck, and H. W. Schreier, "Quantitative error assessment in pattern matching: Effects of intensity pattern noise, interpolation, strain and image contrast on motion measurements," *Strain*, vol. 45, no. 2, pp. 160–178, 2009.
[23] G. Crammond, S. W. Boyd, and J. M. Dulieu-Barton, "Speckle pattern quality assessment for digital image correlation," *Opt. Lasers Eng.*, vol. 51, no. 12, pp. 1368–1378, 2013.
[24] P. Mazzoleni, F. Matta, E. Zappa, M. A. Sutton, and A. Cigada, "Gaussian pre-filtering for uncertainty minimization in digital image correlation using numerically-designed speckle patterns," *Opt. Lasers Eng.*, vol. 66, pp. 19–33, Mar. 2015.
[25] H. Yang, Q. Gu, T. Aoyama, T. Takaki, and I. Ishii, "Dynamics-based stereo visual inspection using multidimensional modal analysis," *IEEE Sensors J.*, vol. 13, no. 12, pp. 4831–4843, Dec. 2013.
[26] G. Busca, G. Ghislanzoni, and E. Zappa, "Indexes for performance evaluation of cameras applied to dynamic measurements," *Measurement*, vol. 51, pp. 182–196, May 2014.
[27] T. Siebert, T. Becker, K. Spiltthof, I. Neumann, and R. Krupka, "High-speed digital image correlation: Error estimations and applications," *Opt. Eng.*, vol. 46, no. 5, p. 051004, 2007.
[28] P. Olaszek, "Investigation of the dynamic characteristic of bridge structures using a computer vision method," *Measurement*, vol. 25, no. 3, pp. 227–236, 1999.
[29] G. Busca, A. Cigada, P. Mazzoleni, M. Tarabini, and E. Zappa, "Static and dynamic monitoring of bridges by means of vision-based measuring system," in *Topics in Dynamics of Bridges* (Conference Proceedings of the Society for Experimental Mechanics Series), vol. 3. New York, NY, USA: Springer, 2013, pp. 83–92.
[30] C. Niezrecki, P. Avitabile, C. Warren, P. Pingle, and M. Helfrick, "A review of digital image correlation applied to structural dynamics," in *Proc. AIP Conf.*, vol. 1253. 2010, pp. 219–232.
[31] K. Schreve, "How accurate can a stereovision measurement be?" in *Proc. 15th Int. Workshop Res. Edu. Mechatronics (REM)*, 2014, pp. 1–7.
[32] E. Zappa, P. Mazzoleni, and A. Matinmanesh, "Uncertainty assessment of digital image correlation method in dynamic applications," *Opt. Lasers Eng.*, vol. 56, pp. 140–151, May 2014.
[33] E. Zappa, A. Matinmanesh, and P. Mazzoleni, "Evaluation and improvement of digital image correlation uncertainty in dynamic conditions," *Opt. Lasers Eng.*, vol. 59, pp. 82–92, Aug. 2014.
[34] R. B. Panerai *et al.*, "Spectrum analysis and correlation," in *Electrical Measurement, Signal Processing and Displays* (Principles and Applications in Engineering). Boca Raton, FL, USA: CRC Press, Jul. 2003, pp. 23-1–23-24.
[35] *Photography—Electronic Still Picture Imaging—Resolution and Spatial Frequency Responses*, document ISO 12233:2014, International Organization for Standardization, Feb. 2014.
[36] A. Donges and R. Noll, "Laser triangulation," in *Laser Measurement Technology* (Springer Series in Optical Sciences), vol. 188. Berlin, Germany: Springer, 2015, pp. 247–278.
[37] T. W. Anderson and D. A. Darling, "Asymptotic theory of certain 'goodness of fit' criteria based on stochastic processes," *Ann. Math. Statist.*, vol. 23, no. 2, pp. 193–212, 1952.
[38] T. Hua, H. Xie, S. Wang, Z. Hu, P. Chen, and Q. Zhang, "Evaluation of the quality of a speckle pattern in the digital image correlation method by mean subset fluctuation," *Opt. Laser Technol.*, vol. 43, no. 1, pp. 9–13, 2011.
[39] C. Cofaru, W. Philips, and W. Van Paepegem, "A novel speckle pattern—Adaptive digital image correlation approach with robust strain calculation," *Opt. Lasers Eng.*, vol. 50, no. 2, pp. 187–198, 2012.
[40] R. I. Hartley and A. Zisserman, *Multiple View Geometry in Computer Vision*, 2nd ed. Cambridge, U.K.: Cambridge Univ. Press, 2004.

Alberto Lavatelli (M'14) received the M.Sc. degree in mechanical engineering from the Politecnico di Milano, Milan, Italy, in 2015, where he is currently pursuing the Ph.D. degree with the Department of Mechanics.

His current research interests include the development of vision-based techniques applied to mechanical and thermal measurements.

Emanuele Zappa (M'10) received the Ph.D. degree in applied mechanics from the Politecnico di Milano, Milan, Italy, in 2002.

He has been a Researcher with the Department of Mechanical Engineering, Politecnico di Milano, since 2001, where he is currently an Associate Professor. He has authored several publications in the field of measurements, with a focus on vision-based techniques, such as digital image correlation, 3-D structured light scanning, and stereoscopy. His current research interests include the development, the improvement, and the uncertainty analysis of the aforementioned techniques, and their application in complex and harsh environments.